DESIGN OF DRIFT TUBE LINACS

D. Young
Midwestern Universities Research Association

A design proposal for a 10 Bev FFAG accelerator has been submitted to the AEC. The proposed injector for this machine is a 200 Mev linear accelerator, which will be discussed here. Since funds for this machine have not yet been provided, no detailed design work has been done. Rather, a set of parameters for the linac has been arrived at.

Before discussing this particular 200 Mev linac, it seems worthwhile to mention other linac work, separate from the actual FFAG injector design, that has been done or is in progress at MURA.

A linac computational program has been developed for the calculation of the frequencies and fields in resonant cavities. A considerable amount of data has come from this program, some of which will be presented here. These data should make the design of drift tube linacs somewhat simpler, by following a "brute force" technique of achieving an optimum in geometry to minimize rf power losses.

Further, a program has been written for the I.B.M. 704 computer to treat the phase motion in linacs. The results of this program have been reported at the Linear Accelerator Conference of April, 1961.* It is planned to write a similar program in the near future to deal with radial motion.

Two additional problems are being investigated theoretically under the direction of J. Van Bladel. These are the problem of beam loading, and the problem of coupling rf power into the resonant cavities. The beam loading

*BNL, IA AvS - 1

aspects of the program will be discussed later in this conference by F. Mills.

Experimentally, two instruments of interest are available. One is a precision frequency cavity which has been used to check the resonant frequencies, and which will be used to check the fields, obtained from the computer calculations mentioned above. Presently, it has been verified that correct frequencies are obtained from the computer.

The other experimental facility is a short section of power cavity which is in the process of being machined. Four tubes, Eimac 3W10000, are available to drive this cavity. These will probably not be used, however, since a tube, RCA 2041, which can deliver about 200 kw of rf power has recently been acquired. This will allow us to power a 70 Mev section of copper-clad cavity of about one meter in length. Hopefully, it will be possible to power larger sections in the future.

The parameters for the 750 kev Cockcroft-Walton preinjector and the parameters for the buncher are given in Table 1. It is felt that

Table 1

Preinjector: Cockcroft-Walton

Energy:	750 kv
Source:	Duoplasmatron
Source Output Current: (Total unanalyzed)	90 ma
Source Output Current: (H^+ only)	70 ma
Emittance at 750 kv	6π millirad - cm
Output Energy Spread	± 0.1%

Buncher:

Output Energy Spread	± 2%
Output Current	60 ma

the proposal of 70 ma analyzed beam from the duoplasmatron ion source is something that can be readily achieved. The 6π cm-mrad emittance seems to be consistent with the figures presented by L. Smith in the preceding report "The New Bevatron Injector".

The parameters for the linac and debuncher are shown in Table 2.

Table 2

Linear Accelerator:

Energy	200 Mev
Input Current in Linac Synchrotron Phase Acceptance	30 ma
Transverse Phase Space Acceptance	10π millirad - cm
Output Current	30 ma
Output Energy Spread	± 0.5%
Output Emittance	0.5π millirad - cm
Repetition Rate	30 cycles/sec
Particle Acceleration Pulse Length	50-200 μs
Duty Factor (including tank build-up time)	0.7 - 1.2%
Peak rf Power	23 Mw
Maximum Average rf Power	275 kw
Total Length	120 m

Debuncher:

Output Energy Spread	± 0.10%
Current Output	30 ma

Of course the achievement of 30 ma output current with 30 ma captured current from the buncher will depend on such things as the design of the quadrupole system. The other parameters are conventional. The 50 μsec output pulse will allow for about 20 to 25 turns of injection into the main machine. If 21 turns of 20 ma beam were captured, the main accelerator circulating beam would be .42 amps. The 20 ma figure allows for losses in the beam transport system. For capture efficiencies of less than 100%, a longer injection pulse would be used. On this basis, the upper limit of 200 μsec for the injection pulse is set. This does not include time for rf build-up in the tank. Including a 150 μsec to 200 μsec build-up time, this gives a duty factor of up to 1.2%.

The linac is to be a six tank system, designed along the lines as indicated by G. W. Wheeler in the preceding report. The general picture of the linac is given in Table 3. Some of the numbers have been changed slightly to take into account the most recent computational runs, but, in general, things have remained quite the same.

The six tank design is chosen so that the entire linac, except for the first tank, which requires about .6 Mw, can be powered by the RCA 7835 type tubes, each of which can deliver 5 Mw pulse power.

There seems to be good reason to keep the first tank short, so it goes only to 10 Mev. The acceleration rate is considered conservative. The 10 Mev section is conventional. The other sections are 23 meters long, and similar, except that, in the last two tanks, the voltage gradient must be made smaller to take into account the falling shunt impedance and reduced efficiency of these structures.

Note that the total power, shown at the bottom of Table 3, is higher than the sum of the theoretical cavity powers. This total power figure includes:

1) Losses on the stems, tuners, and coupling loops.
2) The fact that one cannot achieve the theoretical Q, but something like 80% of this.
3) 1 Mw for beam loading, which seems to be a reasonable figure.

Thus 4 or 4.5 Mw per tank looks like a practical power.

Since the computational method for frequencies and fields has not received wide publication, it will be discussed here.

For φ independent transverse magnetic modes, Maxwell's equations reduce to:

$$\frac{\partial^2 F}{\partial r^2} - \frac{1}{r}\frac{\partial F}{\partial r} + \frac{\partial^2 F}{\partial z^2} + k^2 F = 0$$

where $F = rH_\varphi$, and $k = \omega/c$. F is chosen so that the boundary conditions

Table 3

Linear Accelerator Design Parameters

	Tank No. 1	Tank No. 2	Tank No. 3
Energy Range (Mev)	0.75-10	10-50	50-90
Acceleration Rate (Mv/m)	1.7	1.7	1.7
Tank Length (m)	5.5	23	23
Tank Diameter (m)	1.0	0.94	0.88
Gap to Length Ratio (g/l)	0.25	0.24-.32	0.32-.35
Approximate Drift Tube Diameters (cms)	-	18	14-16
Effective Shunt Impedance (including transit time factor)(megohms/meter)	-	40	50
Theoretical rf Losses (megawatts)	0.6	2.1	1.7

	Tank No. 4	Tank No. 5	Tank No. 6
Energy Range (Mev)	90-130	130-165	165-200
Acceleration Rate (Mv/m)	1.7	1.5	1.5
Tank Length (m)	23	23	23
Tank Diameter (m)	0.82	0.76	0.70
Gap to Length Ratio (g/l)	0.34-.36	0.35-.37	0.33-.37
Approximate Drift Tube Diameters (cms)	13-16	12-14	10-12
Effective Shunt Impedance (including transit time factor)(megohms/meter)	37	28	22
Theoretical rf Losses (megawatts)	2.2	2.3	2.9

Tank Resonant Frequency:	200 megacycles per second
Stable Phase Angle:	26°
Total Accelerating Length:	121 m
Total rf Peak Power Required: (with beam loading)	23 megawatts
Average rf Power at 1.2% Duty Cycle:	275 kw
Number of Drift Tubes:	249
Field Strength not to Exceed 15 Mv/m at any point	

are very simple, namely:

$$\left.\frac{\partial F}{\partial n}\right)_{\text{Surface}} = 0$$

except on the axis, where F itself is zero. The difficulties in solving this equation stem from the fact that the variables are not separable. For the solution, the equation is written in operator form:

$$\mathcal{O}F + k^2 F = 0 \quad .$$

An eigenfunction expansion for the solution is used, in conjunction with a variational principle which applies to this case. This allows the determination of the eigenvalue from the field equations.

$$k_o \leq \frac{\langle F\mathcal{O}F\rangle}{\langle FF\rangle} \quad .$$

This leads to a convergent iterative process, whereby the calculated eigenvalue is substituted back into the equation, giving a new value of F. Through iteration, one can arrive at a stationary solution.

Considerable experience has been obtained at MURA with mesh calculations by a group led by F. Christian. Adapting this technique one obtains from the original differential equation the difference relationship given by:

$$F_{i,j+1}\left(1 - \frac{h}{2r_j}\right) + F_{i,j-1}\left(1 + \frac{h}{2r_j}\right) + F_{i+1,j} + F_{i-1,j} + \left(k^2h^2 - 4\right) F_{i,j} + 0\left(h^4\right) = 0$$

In order to make this process converge faster, convergence acceleration is used. R. Christian has details on this process.

At the present time, the program can handle cylindrical drift tubes with rounded corners and holes with rounded corners. The solution proceeds quite rapidly if one can arrive at a good initial loading of the mesh. With some little experience, good mesh loadings may be had, and the solution requires only a few iterations.

Recently, the program has been modified to handle arbitrary shaped drift tubes, with only minor restrictions. This enable calculations to be done for any drift tube shape presently in existence. However, this program cannot, for example, treat "dumbell" shaped drift tubes.

Results for the drift tube calculations for 50 Mev, 100 Mev, 150 Mev, and 200 Mev are shown in Figs.1,2,3 and 4, respectively. The lines shown are lines of constant F having the same direction as the E lines in the cell. Six parameters are available for optimization, namely:

1) drift tube diameter
2) gap length
3) cell diameter
4) cell length
5) drift tube corner radius
6) resonant frequency

The values of the resonant frequency, the Q, the transit time factor, and the effective shunt impedance are calculated by the computer and indicated in Figs.1, 2,3 and 4.

Consideration of the results of these calculations leads to the graphs presented in Figs.5,6,7 and 8. Here the drift tube diameter,d, is plotted versus the gap length,g, with the parameter,r, the radius of the drift tube corner. Lines on these graphs are for a constant frequency of 200 Mc/s. The numbers adjacent to the points on the curves give the effective shunt impedance at these points. Thus one clearly sees how the effective shunt impedance varies with drift tube diameter, always keeping the gap length such as to maintain resonance at 200 Mc/s. The results shown in Figs. 5,6,7 and 8 are all for an energy of 200 Mev, a constant cavity length L of 84 cm, and various cavity diameters D (in cm).

Note that the curves, as shown, have definite terminations, e.g., for r = 6 cm, one obviously cannot have d less than 12 cm, and to allow for holes in the drift tubes, d cannot even go this small.

It should be apparent that if one can get by with smaller drift tubes, long thin drift tubes give better values for the effective shunt impedance than the shorter, fatter tubes, which suffer from a longer transit time factor. The major losses in the long thin tubes come from power losses on the tubes themselves.

Calculations of this sort have been done for 100 and 150 Mev, and are planned for 50 Mev. With such information, it would seem possible to see quite closely what the parameters of a linac with this type drift tube would be.

As can be seen from Figs. 1,2,3 and 4, raising the energy results in field configurations deviating increasingly from that expected for a TM_{010} mode.

With this problem in mind, a computer program has been written which divides F by r, to obtain H_{φ}. The results of these calculations are shown in Figs. 9,10,11 and 12. The lines as indicated are obtained directly from the computer output. These lines, referred to as "iso-H" lines are not, of course, in the direction of H, (which is perpendicular to the plane of the page), but give magnitudes only. The F values were divided into 14 equal parts, to give 14 iso - H lines. As the energy increases, the field clearly deteriorates, resulting in large H values along the drift tube walls, with consequent high currents and power losses.

These high currents on the drift tubes give rise to two problems. First, it may be necessary to shape the drift tubes to move more of the flux back toward the gap and second, using conventional coupling techniques, it appears difficult to excite the desired field. These two problems must be looked into in greater detail.

This work is continuing. The described program has not been used to its fullest extent and a greater amount of useful data should be forthcoming soon.

Discussion

S. Ohnuma (Yale): How did you get the value of 10π cm-mrad for the linac acceptance?

D. Young (MURA): This is a tentative number, obtained without calculation. We just went to the literature and picked out this number as being reasonable. This number is, of course, subject to change as the design of the system evolves.

R. L. Gluckstern (Yale): Why is the shunt impedance lower in the second tank as compared with the third tank?

D. Young (MURA): This is because in tank 2 the value indicated is not an optimum. A drift tube diameter was chosen such that a quadrupole magnet could be fitted in with no real difficulty, forgetting about conserving rf power there. In tank 3, the shunt impedance is more realistic, close to what the optimum value should be.

I. J. Polk (BNL): I noticed that in the first tank, which runs to 10 Mev, which I assume you isolated because this is one of the most difficult sections, you nevertheless keep the energy gain per meter the same. I should think you would want to reduce this here to achieve a more reliable limit.

D. Young (MURA): I believe that is right, however, we have an extremely powerful tool for determing where the tank is likely to spark, because our computational program gives us the fields at every point. We have in fact made an examination of, not the first tank, but the later tanks, and find that the peak field is somewhere around 8 to 10, in one case I think 12 Mv/meter. This occurs right at the point of curvature on a drift tube, which is cylindrically shaped with a round corner.

I.J. Polk (BNL): I do not know whether this is directly connected with this, but in our case, it would seem that the sparking has something to do with the fact that the drift tube faces are almost flat over a large area. It may not be directly connected with the peak field.

N. D. West (Rutherford): I can agree with that too. It does not look like sparking takes place at the point where you compute maximum fields, but seems to occur on the flat faces.

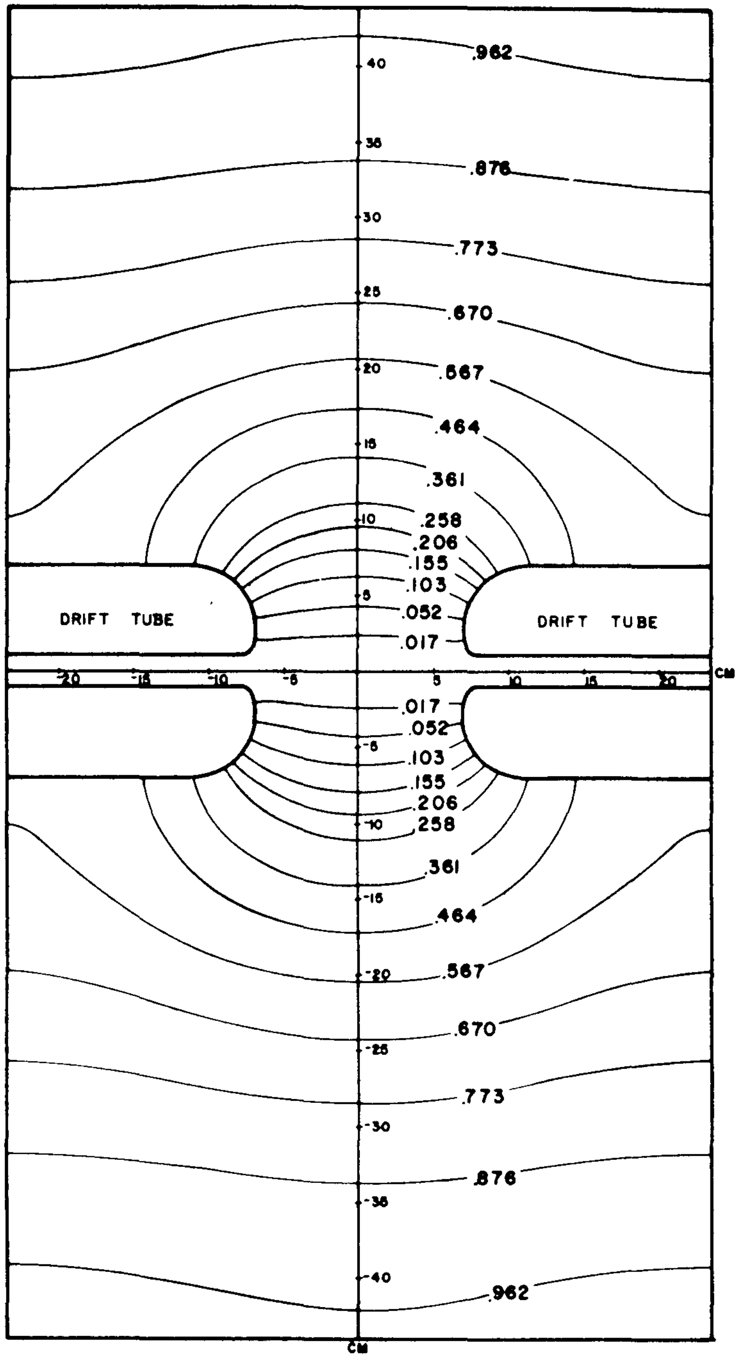

$F = rH$ (Normalized To $5.06 \times 10^{-6} \frac{\text{Joules}}{\text{meter}^3}$)

$f = 200.8$ Mc

$\beta = 0.313$ (49.6 Mev)

$Q = 76{,}900$

$T = 0.800$ (Transit Time Factor)

$ZT^2 = 55.2 \frac{\text{megohms}}{\text{meter}}$ (Effective Shunt Impedance)

F PLOT OF A 50 MEV LINAC UNIT CELL

Fig. 1

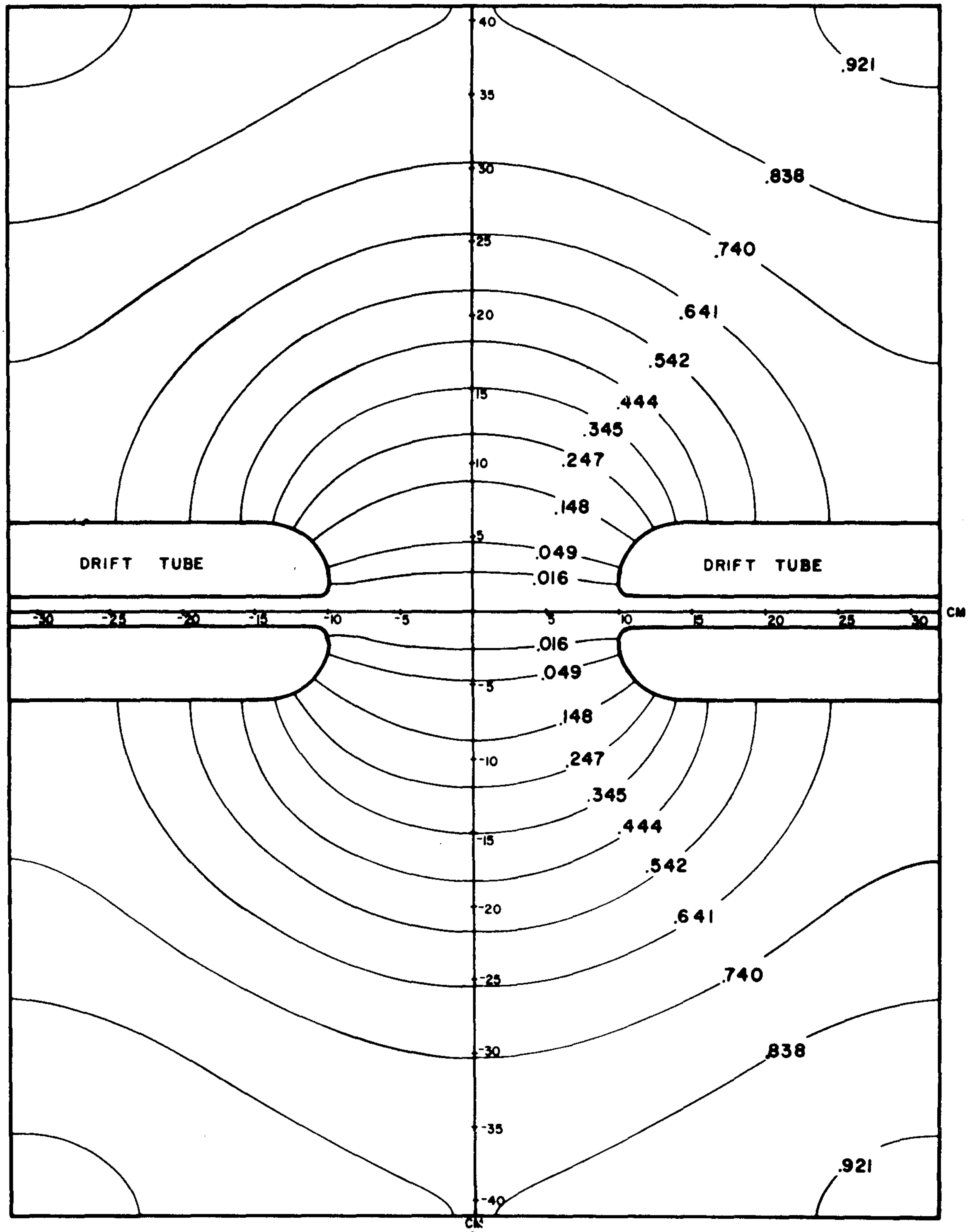

F = rH (Normalized To 5.82 x 10^{-6} $\frac{\text{Joules}}{\text{meter}^3}$)

f = 197.8 Mc

β = 0.427 (99 Mev)

Q = 60,500

T = 0.771 (Transit Time Factor)

ZT^2 = 39.9 $\frac{\text{megohms}}{\text{meter}}$ (Effective Shunt Impedance)

F PLOT OF A 100 MEV LINAC UNIT CELL

Fig. 2

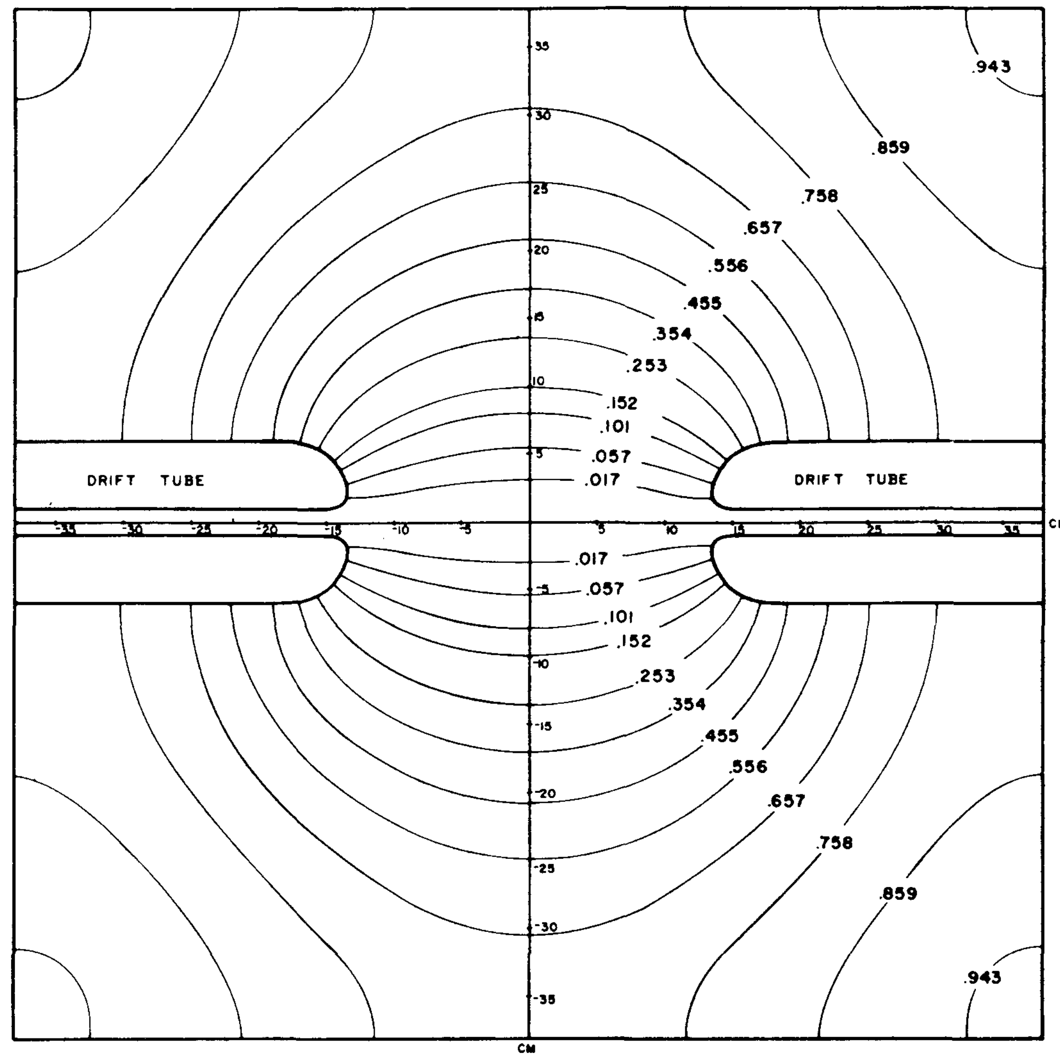

F = rH (Normalized To 6.78 x 10^{-6} $\frac{\text{Joules}}{\text{meter}^3}$) Q = 52,000

f = 199.8 Mc T = 0.702 (Transit Time Factor)

β = 0.5066 (150 Mev) ZT^2 = 26.1 $\frac{\text{megohms}}{\text{meter}}$ (Effective Shunt Impedance)

F PLOT OF A 150 MEV LINAC UNIT CELL

Fig. 3

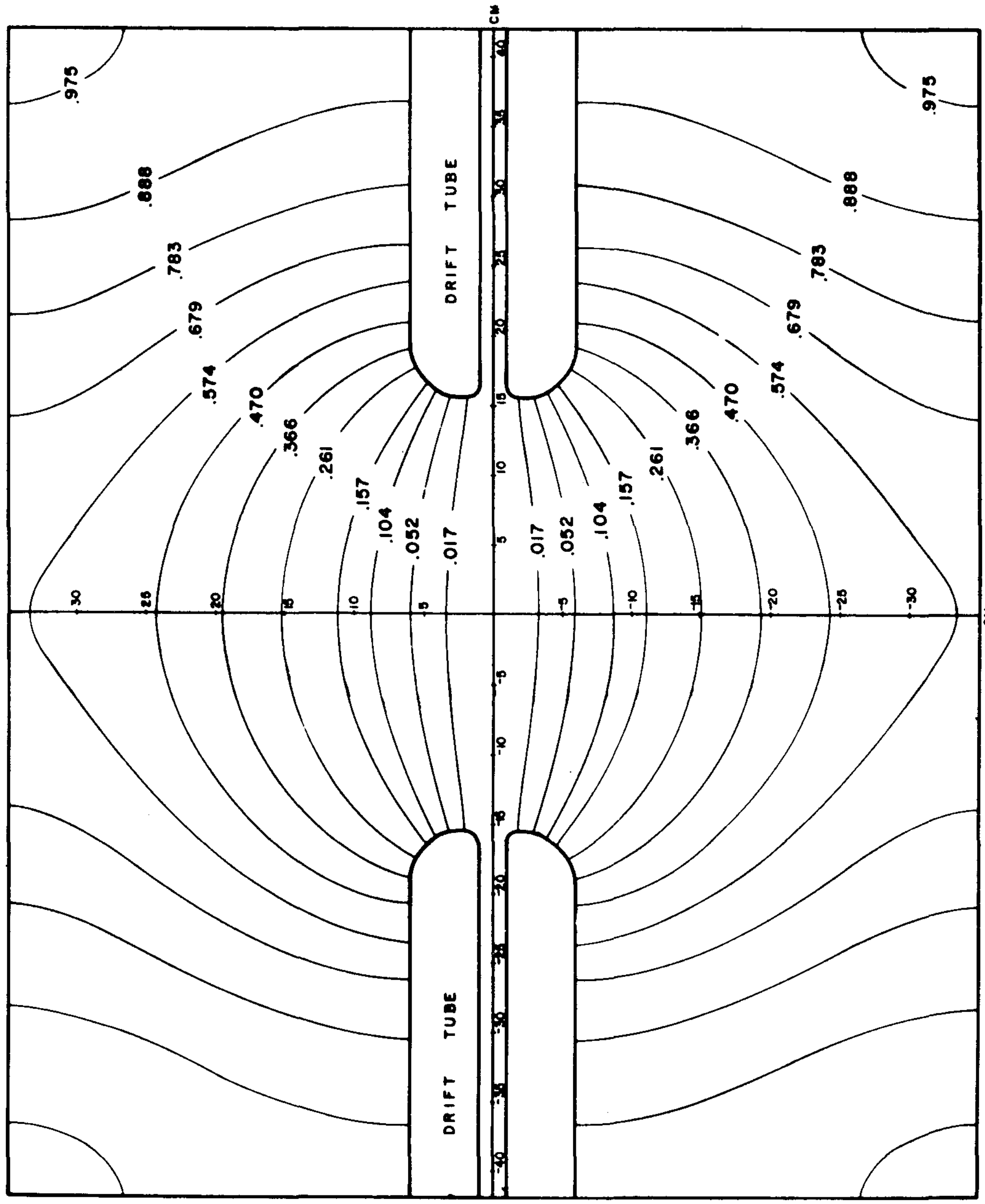

$F = rH$ (Normalized To 7.99×10^{-6} $\frac{\text{Joules}}{\text{meter}^3}$)

$f = 199.4$ Mc

$\beta = 0.560$ (194 Mev)

$Q = 45{,}500$

$T = 0.673$ (Transit Time Factor)

$ZT^2 = 19.2$ $\frac{\text{megohms}}{\text{meter}}$ (Effective Shunt Impedance)

F PLOT OF A 200 MEV LINAC UNIT CELL

Fig. 4

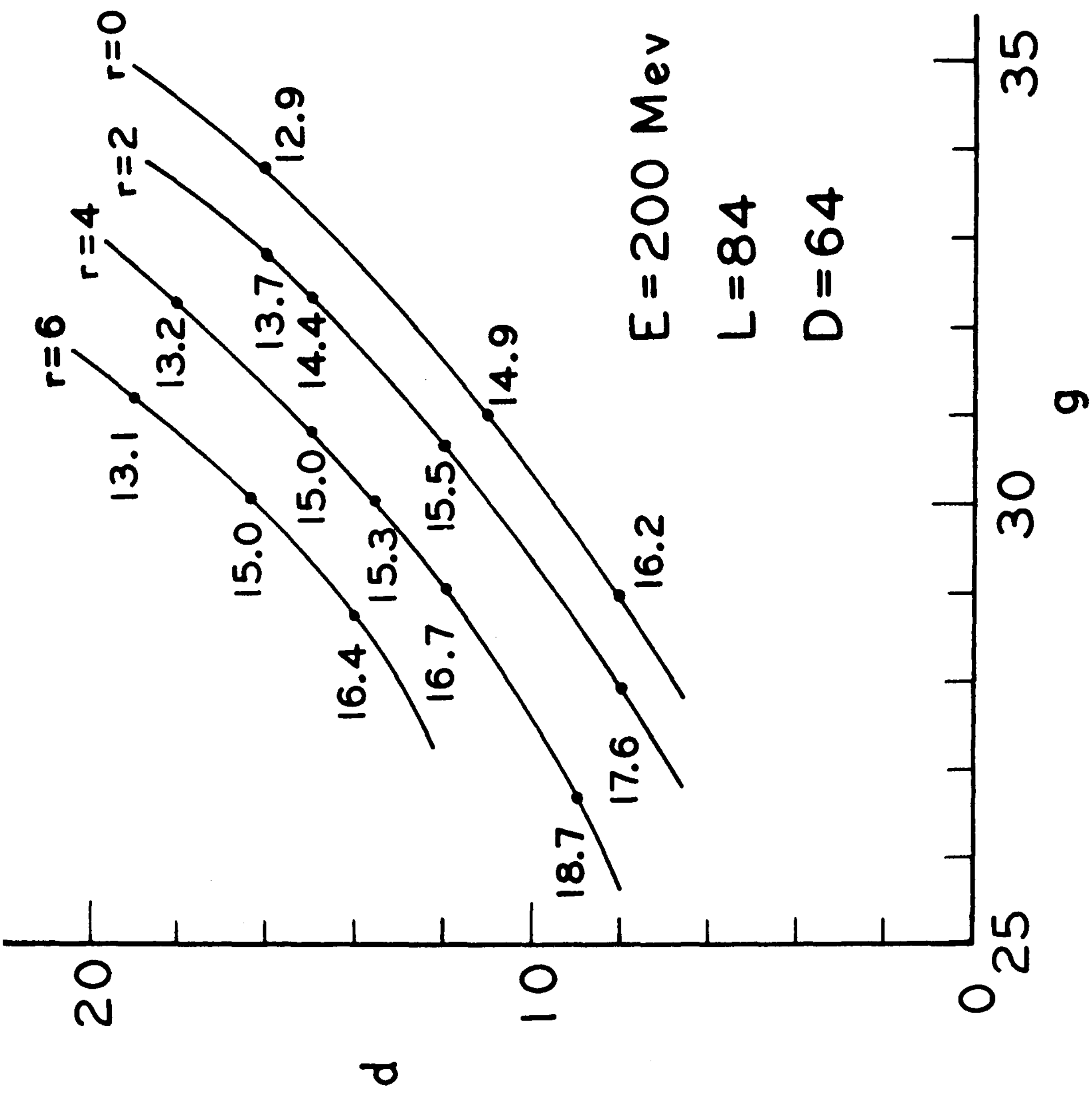
E = 200 Mev
L = 84
D = 64
r=0
r=2
r=4
r=6
12.9
14.9
16.2
13.7
14.4
15.5
17.6
13.2
15.0
15.3
16.7
18.7
13.1
15.0
16.4
d
g
0
10
20
25
30
35

Fig. 5

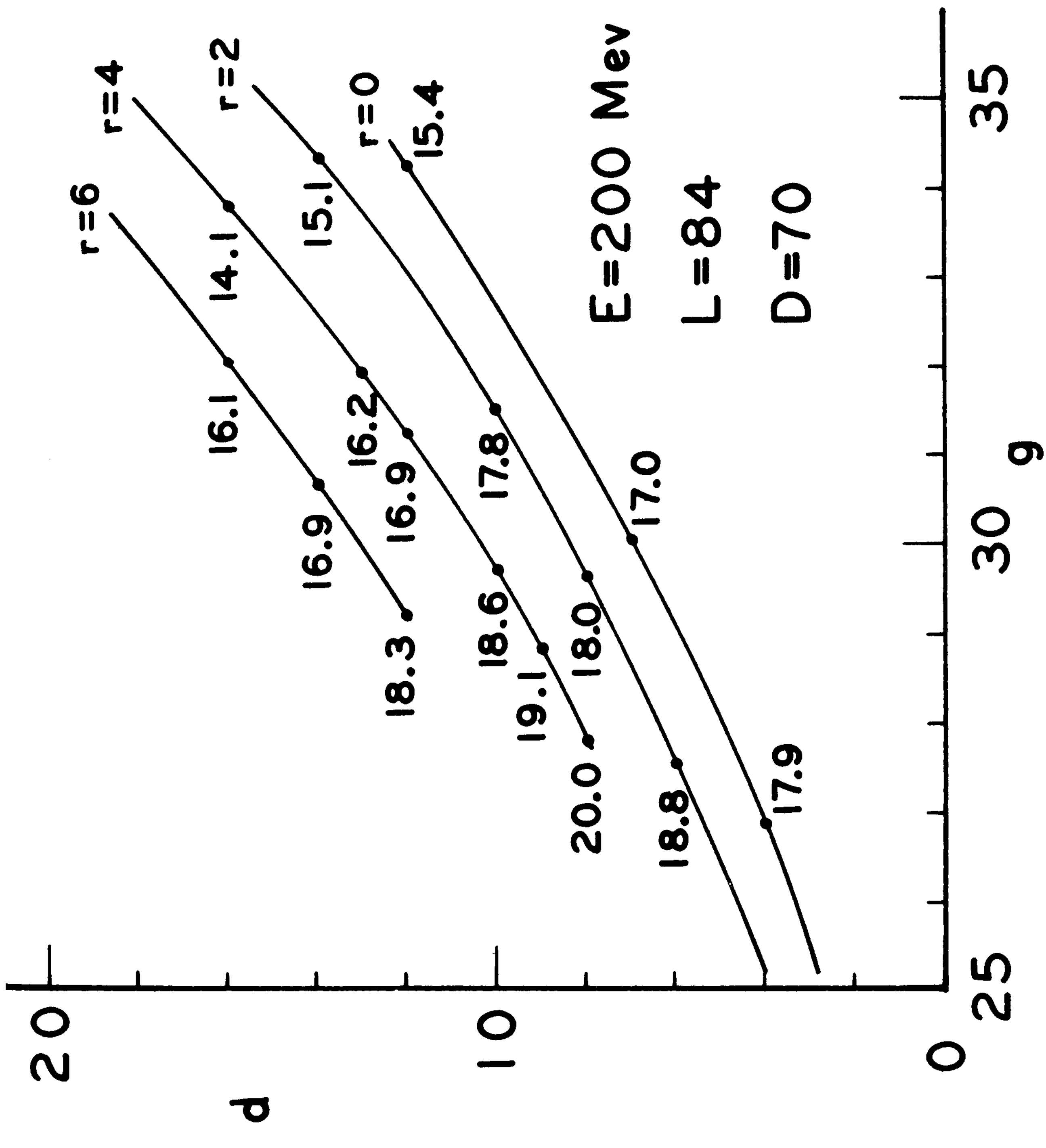
r=6
r=4
r=2
r=0
E=200 Mev
L=84
D=70
18.3
16.9
16.1
20.0
19.1
18.6
16.9
16.2
14.1
18.8
18.0
17.8
15.1
17.9
17.0
15.4
d
g
0
10
20
25
30
35

Fig. 6

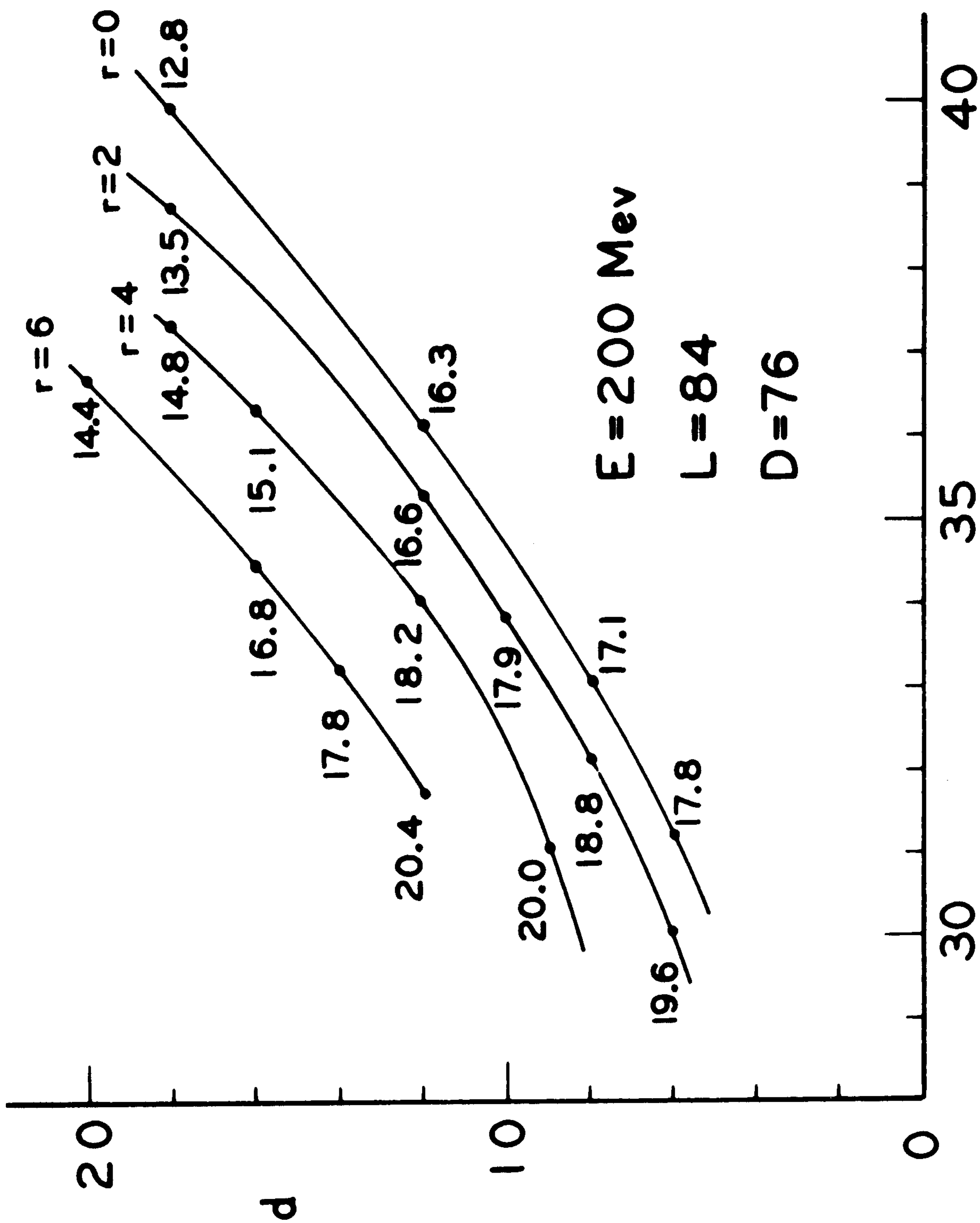
E = 200 Mev
L = 84
D = 76
r = 0
r = 2
r = 4
r = 6
12.8
13.5
14.8
14.4
16.3
15.1
16.6
16.8
17.1
17.9
18.2
17.8
17.8
18.8
20.0
20.4
19.6
g
p
30
35
40
0
10
20

Fig. 7

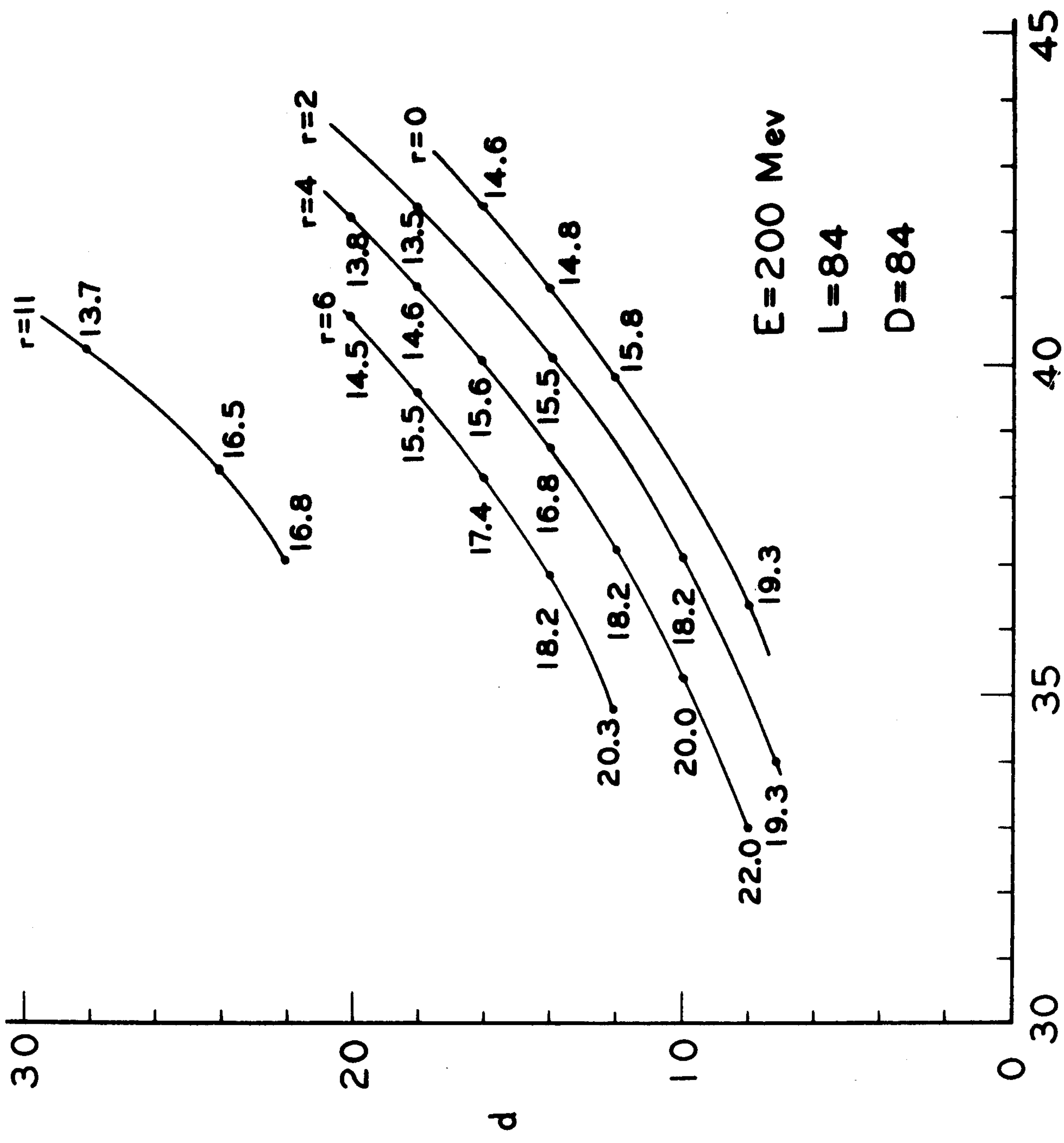
E=200 Mev
L=84
D=84
d
r=11
r=6
r=4
r=2
r=0
13.7
16.5
16.8
14.5
15.5
17.4
18.2
20.3
13.8
14.6
15.6
16.8
18.2
20.0
22.0
13.5
15.5
18.2
19.3
14.6
14.8
15.8
19.3
0
10
20
30
35
40
45

Fig. 8

50 MEV

F-46 MESH NO. 28427 H FIELD.

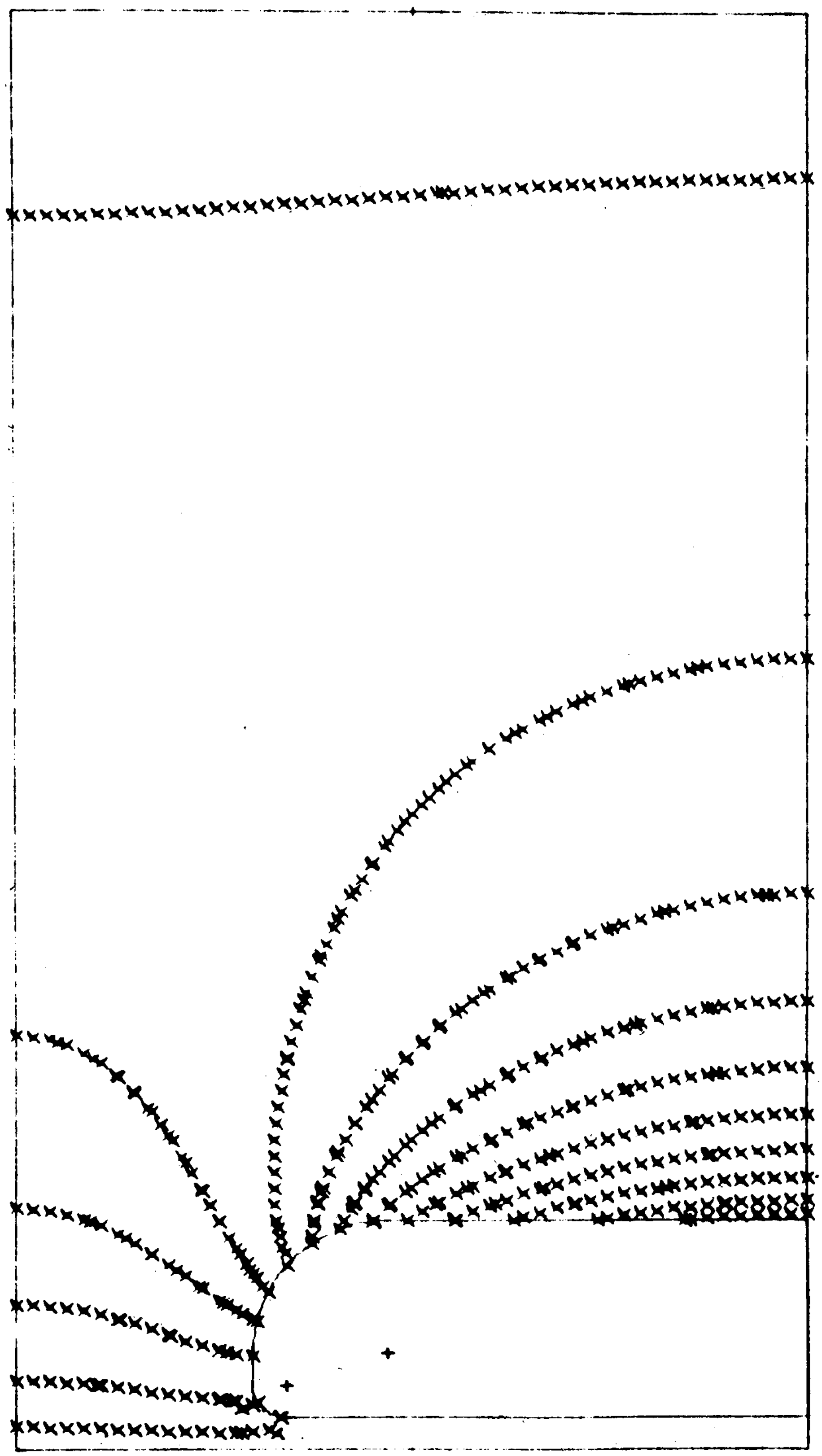

Fig. 9

100 MEV

F-46 MESH NO. 28424 H FIELD.

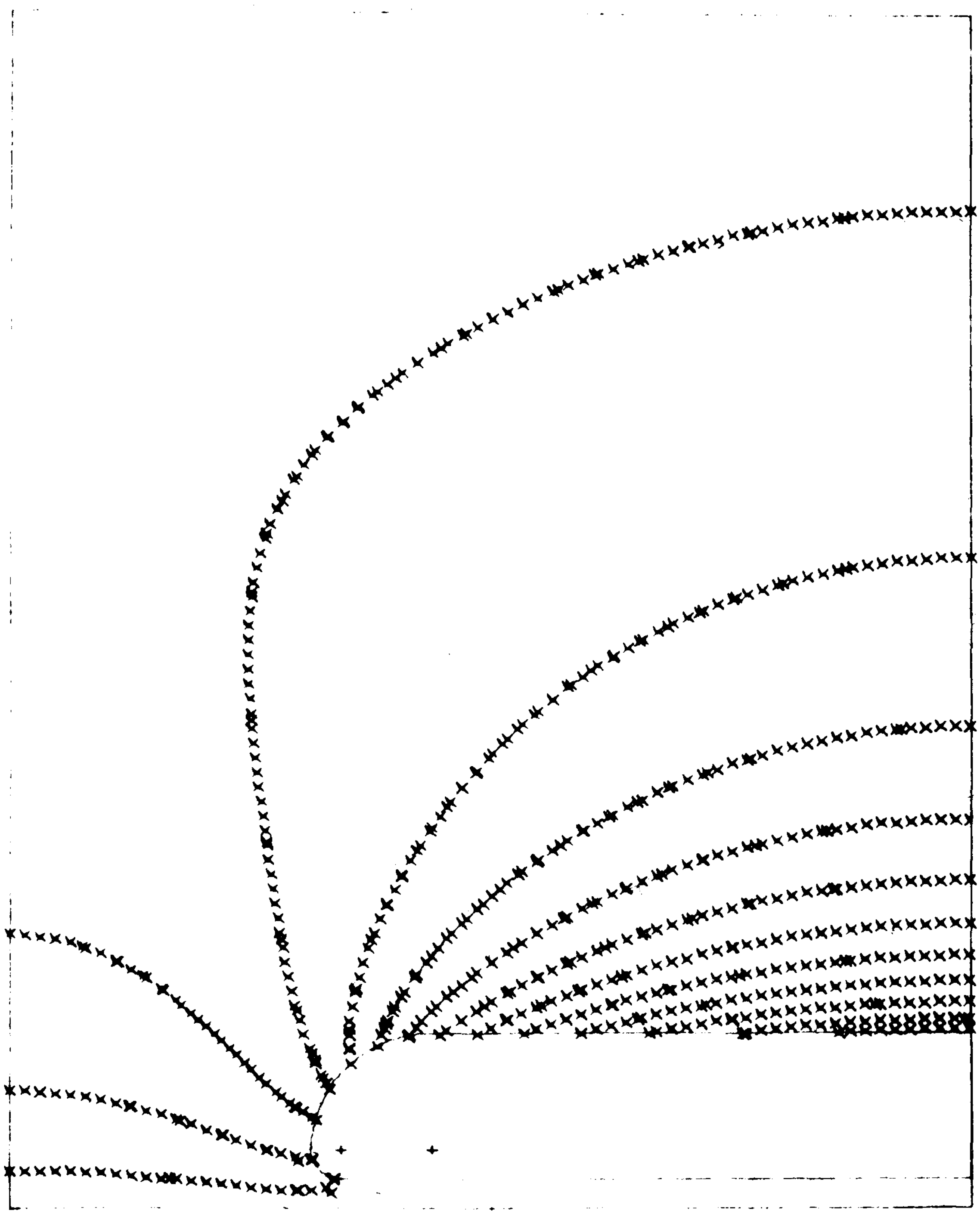

Fig. 10

150 MEV

F-46 MESH NO. 28423 H FIELD.

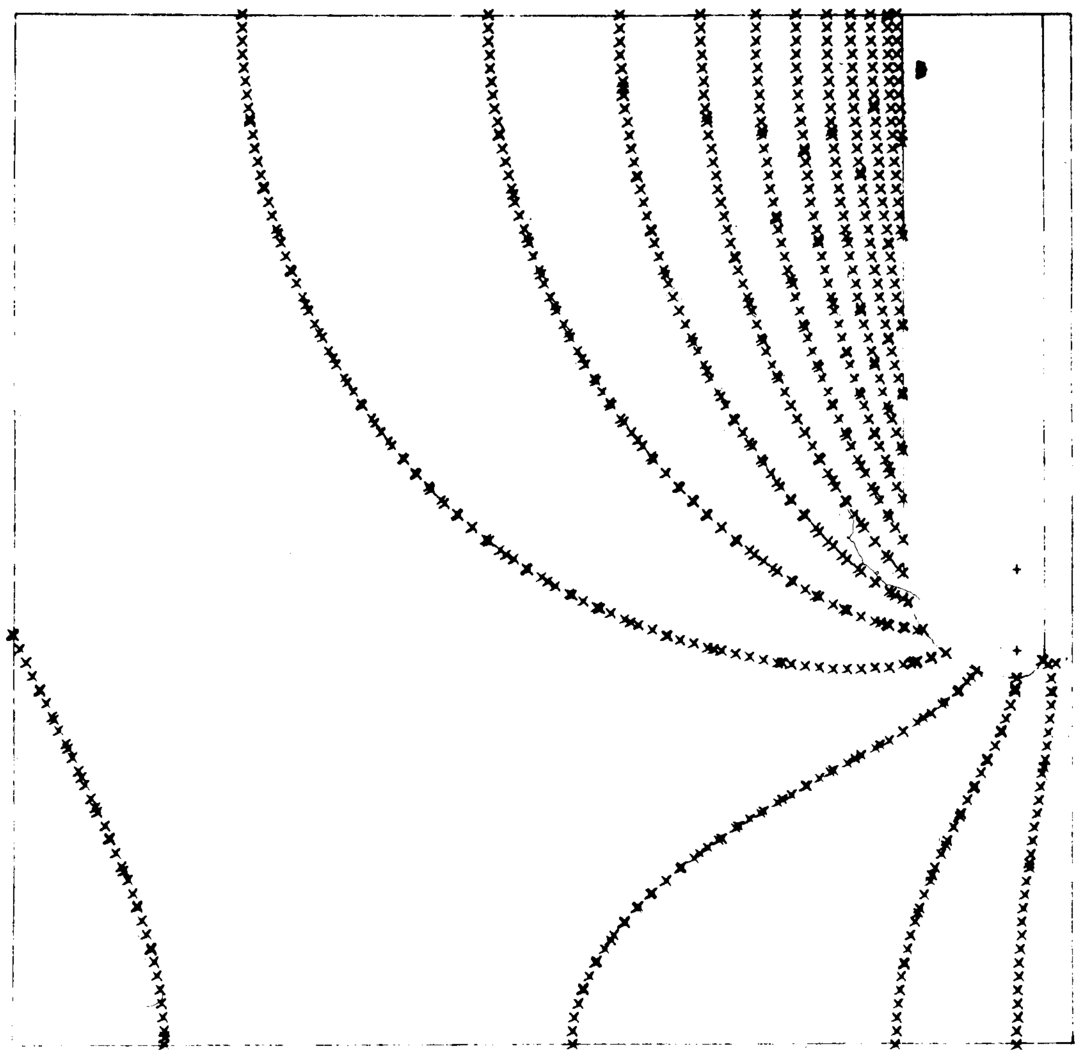

Fig. 11

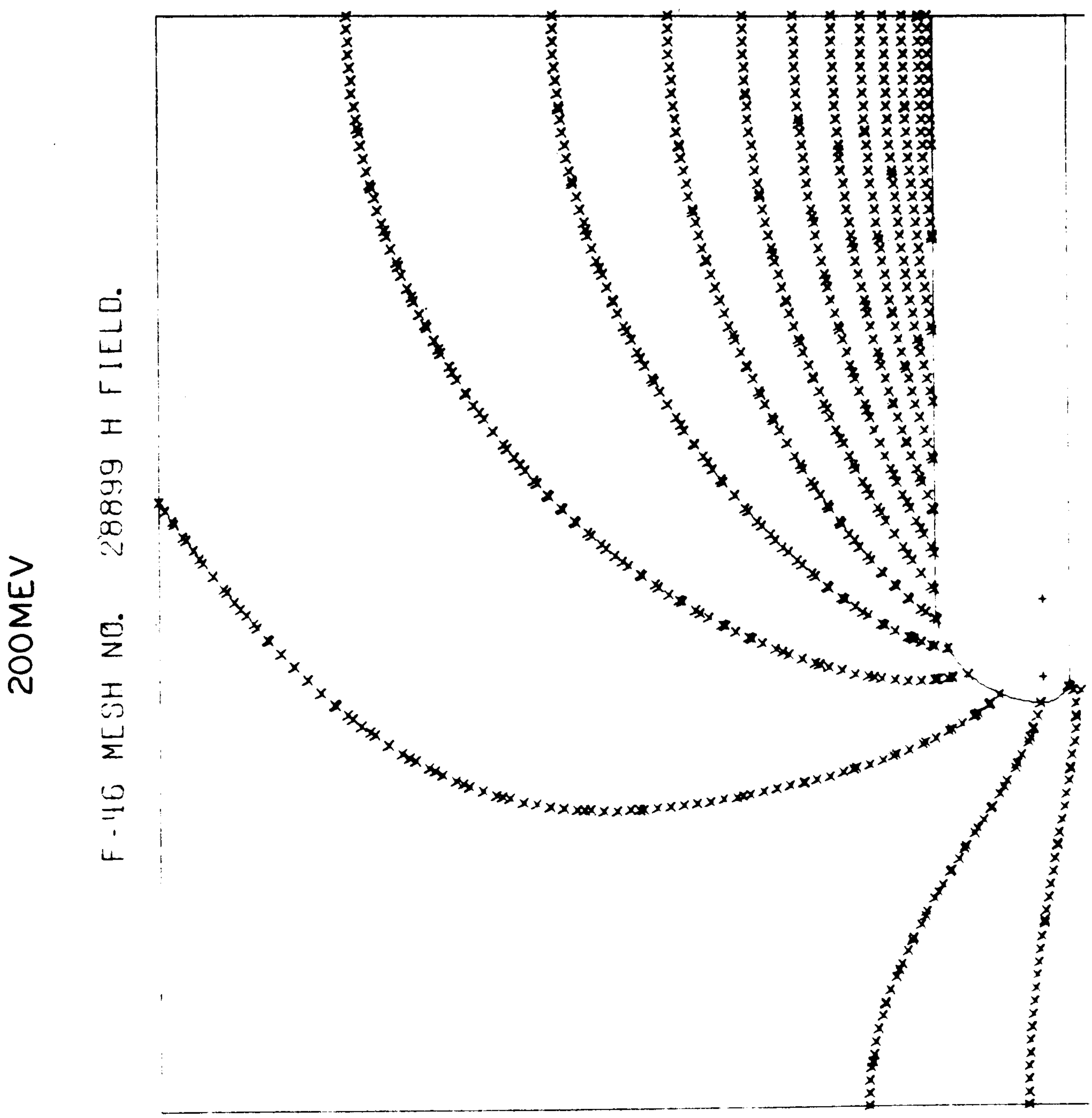

Fig. 12